Electronic materials

Ionic thermoelectric effect in $Cu_{2-\delta}Se$ during phase transition

Bartosz Trawiński[1,*]

[1] *Faculty of Applied Physics and Mathematics, Gdańsk University of Technology, G. Narutowicza 11/12, 80-233 Gdańsk, Poland*

## ABSTRACT

The ionic Seebeck coefficient was studied in copper selenide with $Cu_{1.99}Se$, $Cu_{1.95}Se$ and $Cu_{1.8}Se$ stoichiometry which was synthesized with a melt crystallization method. To measure the ionic Seebeck coefficient of copper ions, $0.15C_6H_{12}N_4CH_3I + 0.85CuI$ solid-state electrolyte was prepared. Electrolyte layers were pressed with copper selenide powder into a sandwich-like structure. At the temperature of 410 K, the materials have ionic Seebeck coefficient values close to each other, about 1100 μV/K. In the case of β-phase structure ($Cu_{1.8}Se$ material), changes in the measured Seebeck coefficient were observed—with decreasing temperature, the ionic thermopower firstly increased reaching about 1230 μV/K and then decreased to 950 μV/K at 355 K. In the $Cu_{1.99}Se$ material, a phase transition to the α-phase was observed during cooling. The ionic Seebeck coefficient values gradually increased from 1030 to 1220 μV/K at 370 K, when the material is in the low-temperature phase. The measured difference between the ionic thermopower of the two phases well matches calculations based on the entropy of the transition (presence part of the Seebeck coefficient) and different activation energies of ionic transport (transport part).

GRAPHICAL ABSTRACT
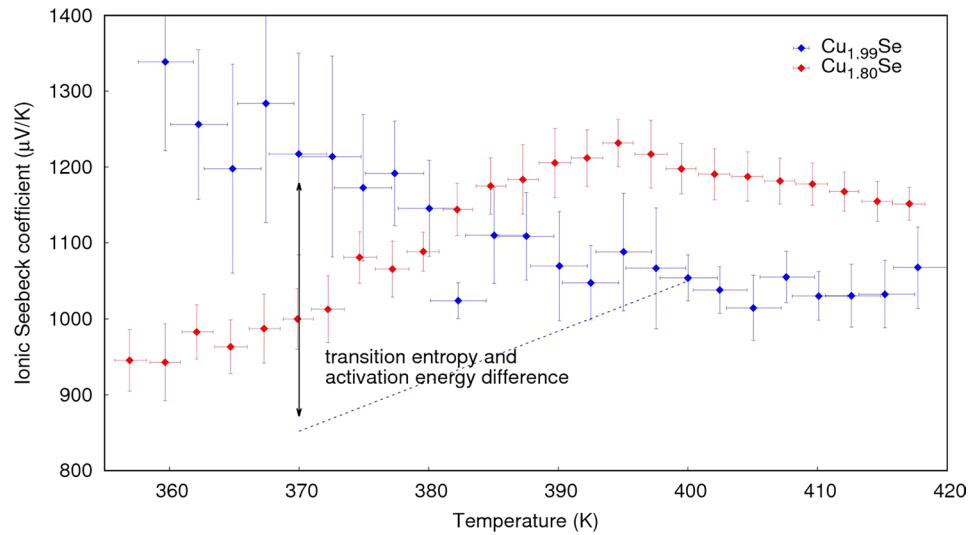
Introduction

The thermoelectric properties of copper selenide (Cu$_2$Se) have been in researchers' interest since the observation of the thermoelectric figure of merit $zT > 1$ in this material in 2012 [1, 2], see, e.g. reviews [3–5]. The material undergoes a phase transition, in which copper sublattice changes from a low-temperature, ordered (albeit low symmetry) α-phase to a disordered (liquid-like) structure with mobile copper cations—β-phase. At the same time, the selenium sublattice maintains its cubic structure. The phase diagram of the two phases is of a limited solubility type. For stoichiometric material, the transition occurs at 411 K. In the case of copper-deficient Cu$_{2-\delta}$Se, a mixed high- and low-temperature phase region exists, and the characteristic high-temperature end of the transition shifts towards lower temperatures with increasing δ value. Copper selenide with stoichiometry Cu$_{1.8}$Se maintains the β structure at room temperature. Phase diagrams can be found in [6, 7].

Recently, arguments were found for the transition being of a continuous type [8]. Others claim that the transformation is of a first-order type, distributed over a temperature range [7]. The λ-shaped DSC peak is then explained with a transition enthalpy of 6.3 kJ/mol [9]. The coexistence of phases is connected to local fluctuations of stoichiometry [10]. A recent study shows a sharp transition in the stoichiometric

copper selenide—the mixed phase region was not observed. Despite the sharp abrupt phase transformation, the Seebeck coefficient changed gradually, which was explained by the structure of electron bands near the transition, which caused the Seebeck coefficient of the low-temperature phase to be similar to the value for the high-temperature phase near the transition temperature [11]. Thus, even in such a "sharp" transition, no step change in the thermoelectric effect is observed, which is characteristic, e.g. for silver sulphide, where the phase transition occurs between unsoluble phases [12, 13]. Previously, in experiments, in which the phase composition was gradually changing, the continuous character of the Seebeck coefficient dependence on temperature was explained by the effective medium theory [7].

The liquid-like behaviour of Cu + ions makes the β-phase a superionic conductor. The electrical ionic conductivity of copper ions reaches 3 S/cm at 673 K, in a stoichiometric polycrystalline material [14]. In the β-phase, there are eight tetrahedral locations (8c Wyckoff position) per unit cell (with 4 Se atoms each). The occupancy of these positions is only about 72%. The rest of the atoms occupy 32f positions enclosing the 8c tetrahedra, and atoms can easily move between these neighbouring positions. The low occupancy of Cu 8c positions in the lattice provides a high probability of hopping between neighbouring sites (or their 32f surrounding positions)—either directly or through almost empty 4b

octahedral positions [15]. The high probability of hopping events results in the high mobility of the Cu^+ ions.

Since the thermoelectric effect is a conjugation of charge and entropy transport, such that the Seebeck coefficient is the amount of entropy transported by a carrier divided by its charge [16]. The thermoelectric effect can occur for different types of carriers. In the case of ions, the transported entropy consists of two parts—molar entropy of the ionic charge carriers (S_{ion}) and heat of transport (Q^*, in J/mol) divided by temperature. Thus, the Seebeck coefficient of ions (α_{ion}) is given by Eq. (1) [17]:

$$\alpha_{ion} = \frac{1}{zF}\left(S_{ion} + \frac{Q^*}{T}\right) \tag{1}$$

F is the Faraday constant, and z is an effective charge of the ion (herein, for Cu^+, $z = +1$). Furthermore, the sum in Eq. 1 can be considered as a sum of the two parts of the Seebeck coefficient: $\alpha_{presence} = S_{ion}/zF$ and $\alpha_{transport} = Q^*/zFT$ [18].

The nature of the heat of transport Q^* is complex. For many compounds, measured values are similar to the activation energy for the ionic conduction mechanism [19]. However, it has been shown by Smith et al. [20], that the heat of transport consists of activation energy for diffusion decreased by its temperature derivative multiplied by the temperature.

The ionic Seebeck coefficient of copper selenide has been measured previously in non-stoichiometric [21] materials. These measurements were performed with a cell designed to give the thermovoltage related only to the heat of transport. In the temperature range of 342–383 °C, the transport part Seebeck coefficient values were in the range of 300–350 μV/K. A sample with $Cu_{1.96}$Se stoichiometry had lower values, 180–210 μV/K. The obtained Q^* values were found to be dependent on temperature and differ from the activation energy values by up to 35%. Another work is the thermotransport of Ag + ions in (Ag, $Cu)_2$Se [22]. These measurements were performed above 200 °C. Furthermore, there has been no study of the total ionic Seebeck coefficient in this material performed so far.

In this paper, the measurement of the total ionic Seebeck coefficient (presence + transport part) in $Cu_{2-\delta}$Se is presented for the first time. The measurements were performed in an interesting temperature region of the phase transition. The characteristic points of the obtained $S_{ion}(T)$ dependence match the beginning and end of the transition. The results are discussed in terms of the thermodynamics of the transition.

Materials and methods

Copper selenide samples with different stoichiometry were synthesized by typical melt crystallization. Cu and Se powders were pressed into pellets and sealed in quartz ampules. The ampules were firstly heated to 650 °C with a 2 °C/min heating rate. After 10 h, further heating to 1175 °C with a rate of 1 °C/min was applied. The material was melted for 3 h and was then cooled down to 700 °C with a 0.5 °C/min rate and was kept at this temperature for 48 h. Further cooling to ambient temperature was performed with a rate of 1 °C/min.

$C_6H_{12}N_4CH_3I$ was synthesized by dissolving 0.9 g of $C_6H_{12}N_4$ in 60 ml of EtOH. About 0.42 ml of CH_3I was added, and the mixture was left overnight. White needle-like crystals were obtained. These were filtered out, washed three times with ethanol and dried. NMR spectroscopy of the obtained material was performed to confirm successful synthesis. The $0.15C_6H_{12}N_4CH_3I + 0.85CuI$ electrolyte was prepared by dissolving 0.088 g of $C_6H_{12}N_4CH_3I$ in MeOH. About 0.336 g of CuI powder was added, and the as-obtained paste was mixed in a mortar until the solvent evaporated. The scheme of the electrolyte preparation is presented in Fig. 1.

Temperature-resolved XRD measurements were performed in a 53–173 °C temperature range. Philips X'Pert Pro diffractometer with CuKα radiation (1.542 Å) was used. Each scan was performed after 5 min stabilization time in each temperature. The temperature was measured with an additional thermocouple placed at the bottom side of the sample holder for accurate temperature measurement. Additionally, room temperature measurements were performed after the synthesis of the samples with a Bruker X2 Phaser diffractometer.

The differential scanning calorimetry (DSC) measurement was performed under an argon atmosphere with a flow rate of 60 ml/min in the temperature range of 35–250 °C (with a heating rate of 10 °C/min) using a NETZSCH DSC 204 F1 Phoenix calorimeter.

The sample for ionic properties measurements was made by pouring 0.035 g of the electrolyte, 0.8 g of hand-milled Cu_2Se and again 0.035 g of the electrolyte into a pressing die with 6-mm diameter and pressing
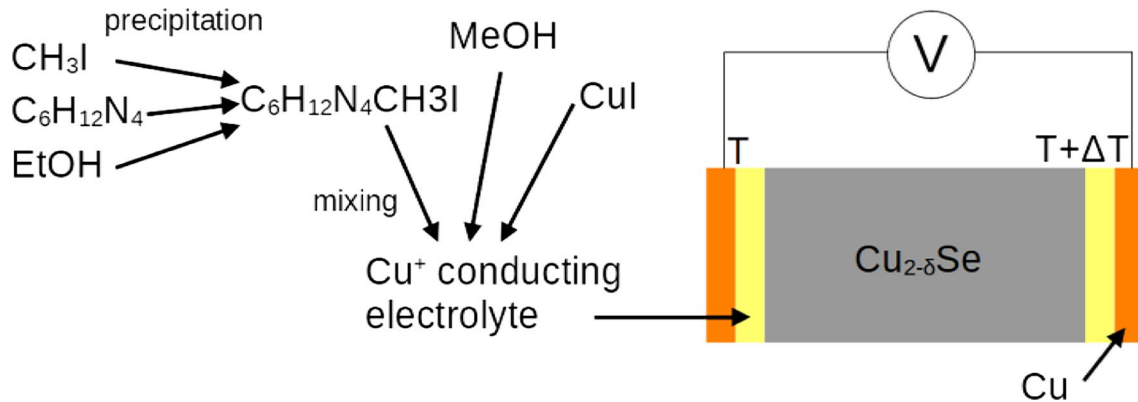
Figure 1 Graph of the electrolyte synthesis and scheme of the circuit for the ionic Seebeck coefficient measurement.

with a pressure of 1.73 GPa. The copper selenide was milled shortly, to maintain the largest possible grains in a compressible powder. The copper selenide powder and Cu_2Se–electrolyte pellets were observed with the FEI Quanta FEG 250 scanning electron microscope with an ETD secondary electrons detector. Elemental composition was analysed with energy-dispersive X-ray spectroscopy using EDAX Genesis APEX 2i with an ApolloX SDD spectrometer. The spectra were analysed with Edax TEAM software. Then, fragments of the copper plate were attached to these surfaces with copper paste CU5056 from Dycotec Materials. The paste required reduction after application, which was performed in a hydrogen atmosphere at 130° for 10 h.

The ionic Seebeck coefficient was measured in a self-made apparatus. Accuracy of the setup was checked with a measurement of the total Seebeck coefficient of Cu_2Se (sample not investigated in this study), the result is provided in the Supplementary material. The scheme of the measurement circuit is presented in Fig. 1. The sample–electrolyte–copper assembly was pressed against the gradient heater on one side using a sharpened screw on the other side. The gradient heater was electrically isolated from the sample assembly. Voltage was measured with thin copper wires attached to the copper plates at two ends of the sample. Temperatures of the two sides of the sample were measured with thermocouples being in contact with the outer surfaces of the electrolyte. Keysight 34970A units were used for voltage and temperature measurement. The ionic Seebeck coefficient was measured in steady-state conditions. Before the measurement started, the sample was equilibrated in the measurement cell with a temperature set to 420 K. Then, the ionic Seebeck coefficient was measured in

the range of 420–340 K set temperature values. The measurement was performed during cooling to avoid overshooting the set temperature by a furnace heater. For each measurement point, the following procedure was enforced. First, the temperature was set on the furnace controller. Then, the system was left to reach the set temperature and stabilize; the total cooling and stabilization time was set to 50 min. After that, a gradient heater was turned on, changing the temperature difference across the sample from − 1.7 to + 1.7 K for $Cu_{1.99}Se$ and from − 0.6 to + 0.6 K for $Cu_{1.8}Se$. The heater remained turned on for 60 min. After that, the sample was stabilized in a turned-off heater regime for 40 min, and the procedure was repeated for the next temperature point.

Results and discussion

Room temperature XRD measurements were performed in the 2θ range of 5–70° to evaluate the.

$Cu_{2-\delta}Se$ synthesis results. Diffraction patterns, provided in Fig. 2, confirm that sample $Cu_{1.99}Se$ has α-phase structure, matching the 47-1448 ICOD pattern of Cu_2Se. The $Cu_{1.8}Se$ sample has a β-phase structure; the pattern matches the 71-0044 $Cu_{1.8}Se$ record. The $Cu_{1.8}Se$ is essentially the same material as Cu_2Se; the off-stoichiometry is noted to emphasise that at room temperature, materials with $Cu_{1.8}Se$ and Cu_2Se stoichiometry have different structures, β and α structures, respectively. Additional small peaks in the $Cu_{1.8}Se$ reference pattern result from planes with high indices' values and were not recorded in this experiment due to lower resolution. NMR spectroscopy was done after the synthesis of $C_6H_{12}N_4CH_3I$
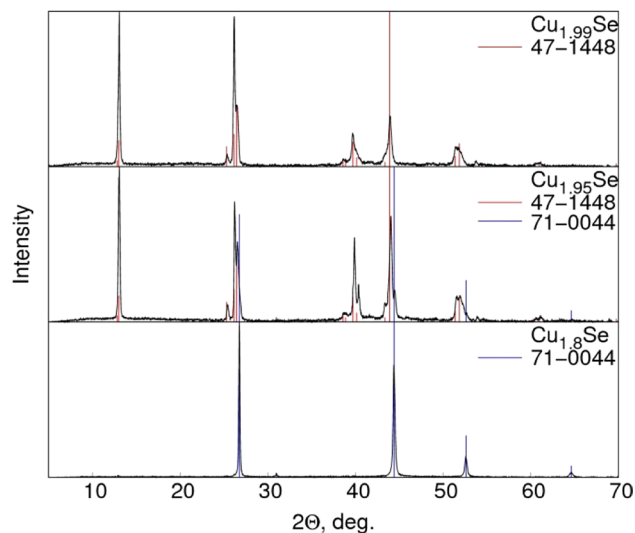
Figure 2 Room temperature XRD patterns of the investigated samples (black lines). Matched patterns from the ICOD database are shown with red (47-1448) and blue (71-0044) lines.

to check the output. The obtained spectrum is 1H NMR (CD$_3$OD, δ ppm): 2.63 (s, 3H, N$^+$–CH$_3$); 4.58 (d, J = 12.7 Hz, 3H); 4.74 (d, J = 13.2 Hz, 3H) and 5.14 (s,

6H). This spectrum confirms that the compound with the expected structure was synthesized. Needle-like shape and white colour of the obtained crystals are expected for this salt.

Figure 3 shows the copper selenide powder, Cu$_2$Se–electrolyte surface and the sample assembled into the measurement cell.

The composition of the copper selenide obtained was evaluated with energy-dispersive X-ray spectroscopy (EDX). For the Cu$_{1.99}$Se, the Cu:Se ratio turned out to be equal to 1.96 ± 0.08. High-temperature X-ray diffraction was performed to determine the phase transition temperature range. Results are presented in Fig. 4a. Diffraction patterns are presented with a scattering angle on the horizontal scale and intensity with presented in colour. The vertical scale shows the temperature, at which the patterns were acquired. In the high-temperature region, a single main maximum is observed at 26.3°. In the low-temperature range, this maximum splits due to lower symmetry. Consequently, in the mixed-phase transition region, a shift of the maxima positions is observed. The beginning and end of this shift marks also the temperature limits of the phase transformation. Herein, the transition

Figure 3 **a** SEM image of Cu$_{1.99}$Se powder, also representative of other samples; **b** cross-sectional view of the electrolyte layer on the copper selenide (representative image of another sample, not used in this study); **c** close-up view of the electrolyte and **d** photograph of the sample assembled in the measurement cell.
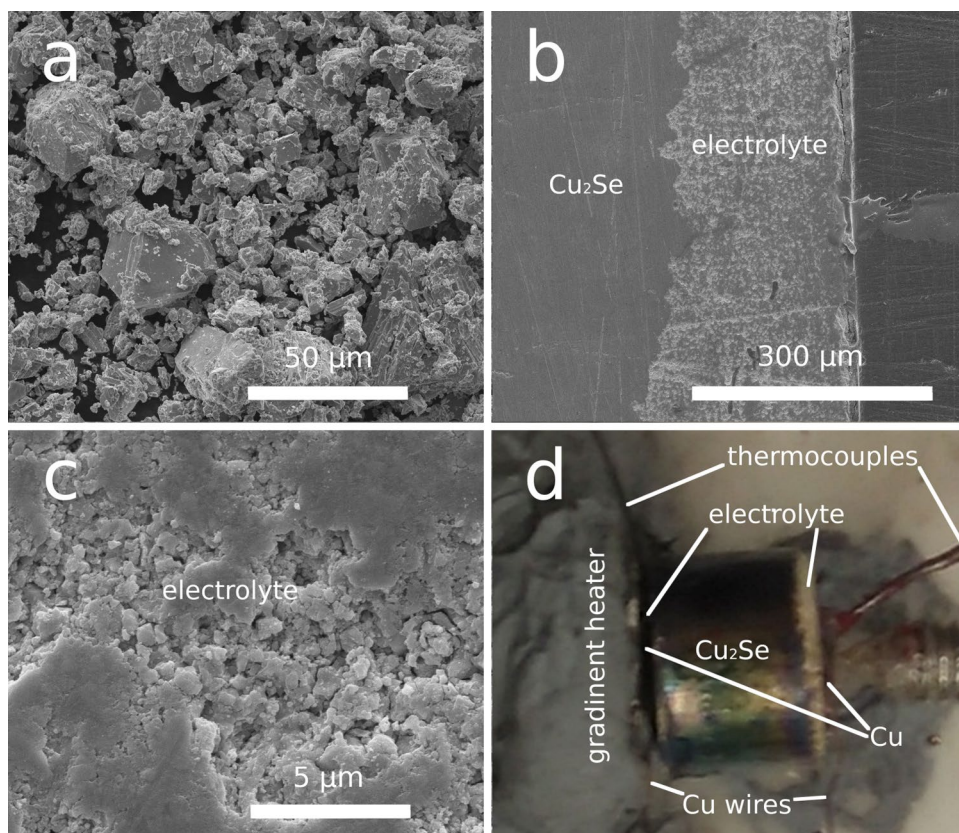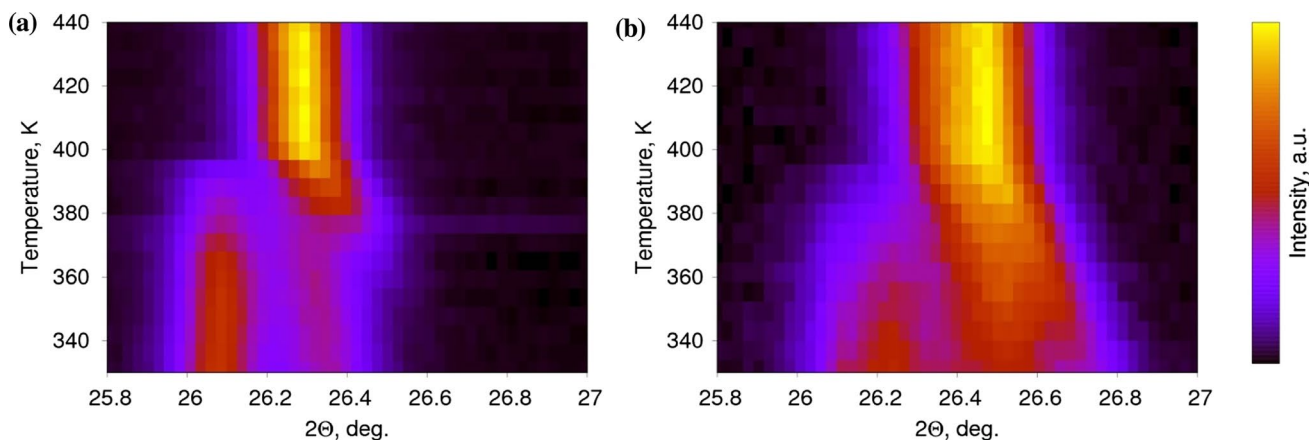
Figure 4 Temperature-resolved X-ray diffraction of **a** $Cu_{1.99}Se$ material and **b** $Cu_{1.95}Se$ material.

is observed between 370 ± 5 and 405 ± 5 K. The lower temperature is sensitive to stoichiometry and matches the Cu:Se ratio of 1.986–1.989, according to the phase diagram [7]. The determined Cu:Se ratio value is close to 2, which was used for the sample synthesis. Selected high-temperature patterns are compared to the low-temperature results in the Supplementary material. Additionally, the results of the DSC measurements are provided therein. An influence of the process' kinetics is visible in that data.

For the next sample with the intended Cu:Se ratio of 1.9, the EDX analysis resulted in a measured value of 2.02 ± 0.11. The high-temperature XRD patterns (Fig. 4b) show that the phase transition takes place in a wider temperature range and, at the low-temperature side, is not completed in the investigated temperature range. The latter is indicated by increasing intensity of the 26.2° maximum. The high-temperature onset of the phase transition occurs at the temperature of 395 ± 5 K. This suggests that the actual composition may be about $Cu_{1.95}Se$, and the material will be referred to with this formula.

The Cu:Se ratio in the $Cu_{1.8}Se$ sample, evaluated with EDX, turned out to be 1.84 ± 0.08. Considering that at room temperature, the material consists of the β-phase only, the real stoichiometry should be closer to $Cu_{1.8}Se$ rather than $Cu_{1.9}Se$. During the synthesis, reactants were taken in the stoichiometry of $Cu_{1.8}Se$.

The ionic thermoelectric effect was investigated in a measurement cell with electron-blocking electrodes, reversible for Cu^+ ions. An exemplary measurement of the ionic Seebeck coefficient in a single temperature point is provided in Fig. 5. Temperature difference with the gradient heater turned off (ΔT_0) and voltage

(U_0) was taken from an average of stable values before and after applying the gradient heater. Values of the temperature difference with gradient heater on (ΔT_1) and the corresponding voltage (U_1) were taken from the stable voltage region. The observed Seebeck coefficient was calculated using Eq. (2).

$$\alpha_{\text{obs}} = \frac{U_1 - U_0}{\Delta T_1 - \Delta T_0} \qquad (2)$$

Standard deviation was taken as the uncertainty of ΔT_0, ΔT_1, U_0 and U_1. The uncertainty of the Seebeck coefficient was calculated from those deviations using the maximal uncertainty method. Uncertainty of the measurement temperature (horizontal bars in Fig. 6) represents the difference between the average temperature recorded at the cold end of the sample with the gradient heater off and the maximal temperature at the hot end with the gradient heater on.

Apart from these stable voltage values, one can identify at least two different effects when the temperature difference across the sample changes. Notice that the first measurement point after the gradient heater is turned on (time = 51 min) has an increased voltage value. Then, the voltage decreases, and after about 1.5 min (three measurement points) after turning the gradient heater on, the voltage raises towards the value, which is stable for the rest of the time (about 50 min). When the gradient heater is turned off (time = 111 min), symmetrical effects are observed. When the heater is turned on, the temperature of the sample slightly increases, shifting the equilibrium phase composition of the material. It has been observed that when copper selenide is out

Figure 5 Exemplary time evolutions of the temperature difference and voltage recorded during the measurement of the ionic Seebeck coefficient in a single measurement point (Cu$_{1.99}$Se, 404 K). The gradient heater was turned on at time = 51 min and turned off at 111 min.
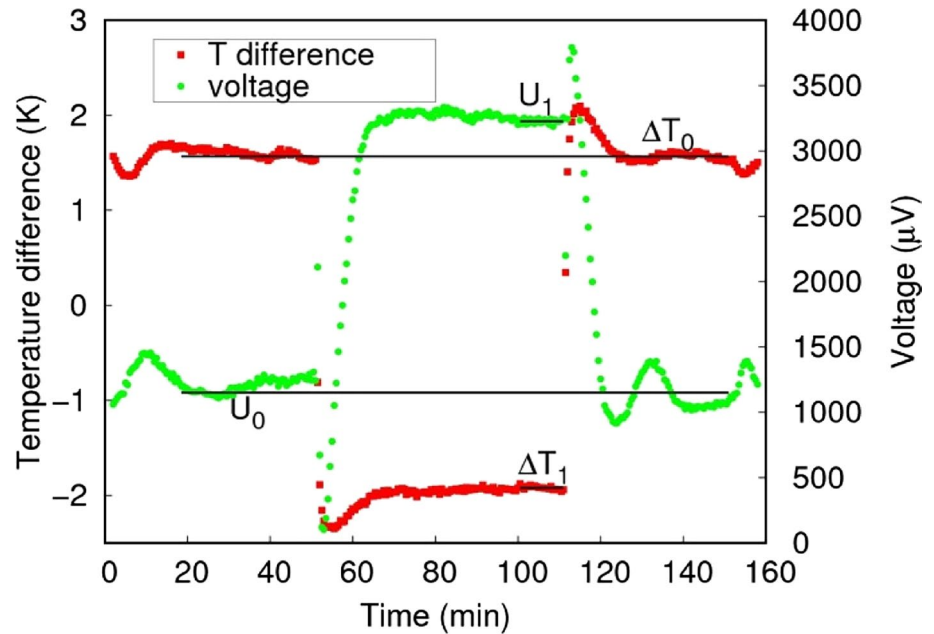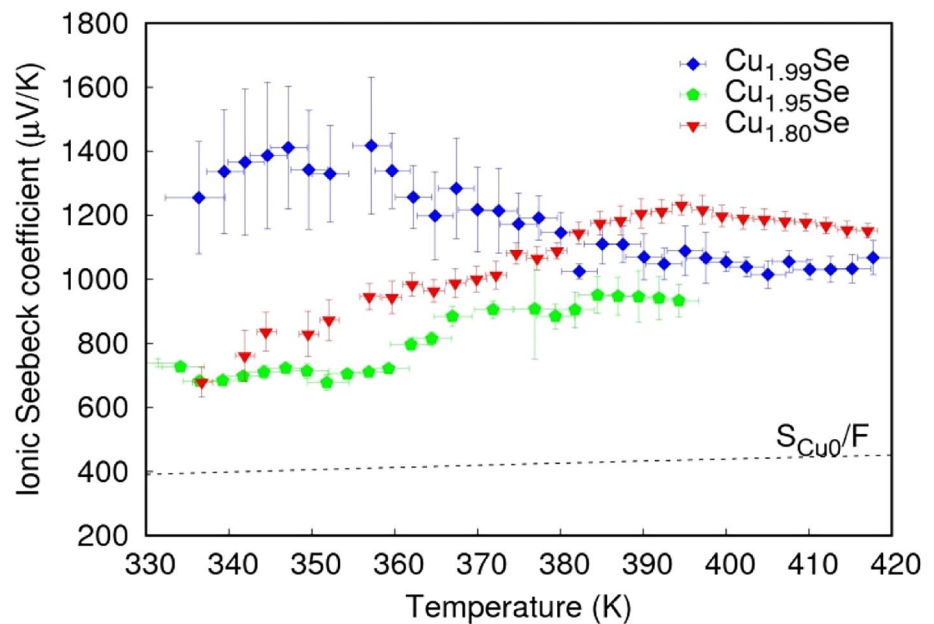

Figure 6 Ionic Seebeck coefficient of the investigated Cu$_{2-\delta}$Se samples. The dashed line shows S_{Cu0}/F values used for calculations.

of its equilibrium phase composition (due to kinetic limitations of the phase transformation), a significant change in the electronic Seebeck coefficient occurs [23]. It is possible that the bidirectional voltage changes observed herein are also related to the kinetic limitation of the small change of phase composition taking place. These effects are in contrast with the "giant" electronic Seebeck coefficient, which was found to be stable in time under constant temperature and temperature gradient conditions [24].

This work focuses on the ionic Seebeck effect measured in stable conditions; thus, the unstable effects are not analysed herein. According to Wagner's derivation [17], the Seebeck coefficient observed in such a system in steady-state conditions (α_{obs}) is given by Eq. (3) (Eq. 43 in ref. [10]).

$$\alpha_{obs} = \frac{1}{zF}\left(S_{Cu^0} - S_{Cu^+} - \frac{Q^*}{T}\right) - \alpha_{Cu} = \frac{S_{Cu^0}}{zF} - \alpha_{ion} - \alpha_{Cu}$$

(3)

S_{Cu0} is the molar entropy of elemental copper, and S_{Cu+} is the molar entropy of copper ions in Cu_2Se. For Cu^+ ions, $z = +1$. α_{Cu} is the Seebeck coefficient of copper wires used in the cell.

For data analysis, $\alpha_{Cu} = 1.5$ µV/K value was taken. The molar entropy of copper was calculated using Eq. (4), taking the standard molar entropy of copper 33.15 J/(mol K) and heat capacity of copper $c = 24.14$ J/(mol K).

$$S_{Cu^0}(T) = S^0_{Cu^0} + c \ln \frac{T}{273.16K} \qquad (4)$$

Figure 6 shows the calculated values of the ionic Seebeck coefficient. A line representing S_{Cu0}/F values is added.

At a high-temperature regime, when the investigated materials are in the high-temperature phase, their values of the ionic Seebeck coefficient are close to each other. This is in agreement with an assumption made by Mostafa et al. [25], that the molar entropy of ions in superionic materials is independent of off-stoichiometry. In the case of the $Cu_{1.99}Se$ sample, in the high-temperature region, the Seebeck coefficient is equal to c.a. 1030 µV/K at 410 K. With the decreasing temperature, the thermopower increases, reaching about 1220 µV/K at 370 K, which is when the material reaches 100% α-phase composition. The ionic Seebeck coefficient further increases up to 1410 µV/K; however, the uncertainty gets high as a result of the high resistivity of the sample. In the $Cu_{1.8}Se$, α_{ion} firstly increases from 1150 to 1230 µV/K with decreasing temperature (from 420 to 395 K). Then, a more significant decrease is observed. A decrease in the ionic Seebeck coefficient with decreasing temperature occurs also in the $Cu_{1.95}Se$ sample above 360 K, showing that its ionic thermoelectric effect is dominated by the β-phase. This is a result of the higher ionic conductivity of the β-phase. While the temperature decreases below 360 K, the Seebeck coefficient stops decreasing due to an influence of the α-phase with higher ionic thermopower. According to the lever rule, at 360 K, the content of the α-phase is roughly 60%. In the case of $Cu_{1.99}Se$, this proportion is reached only about 5 K below the high-temperature onset of the transition. Consequently, the properties of the α-phase influence the $Cu_{1.99}Se$ material during almost the whole transition.

The entropy change of Cu^+ ions related to the $\alpha \rightarrow \beta$ structural phase transition can be estimated. It is herein assumed that all of the transition enthalpy ΔH

contribute to the increase in Cu^+ ions entropy. For simplest calculations, it can be assumed that at considered 411 K temperature, the total Gibbs energy change is equal to zero: $\Delta G = \Delta H - T \Delta S = 0$. For the stoichiometric material, the transition enthalpy ΔH equal to 6.3 kJ per mole of Cu_2Se gives 3.15 kJ per mole of copper ions. Dividing this value by the transition temperature of 411 K and the Faraday constant, the value of the related change in the Seebeck coefficient turns out to be equal to 79 µV/K. The β-phase presence part of the Seebeck coefficient is higher than that of the α-phase at the same temperature by 79 µV/K. The transport part of the ionic thermopower should be also considered. This value is equal to E_a/T, where E_a is the activation energy for ionic conductivity. The energy barrier is equal to 0.14 eV in the high-temperature phase. This value is related to the hopping mechanism between Cu lattice positions [26]. Ionic conductivity in the α-phase was investigated by Horvatic et al. [27]. The apparent activation energy for the ionic conductivity mechanism was found to be 0.29 eV. In this phase, two mechanisms are present: interstitial defect generation and hopping with energies equal to 0.23 and 0.41 eV, respectively [28]. Taking the 0.14 and 0.29-eV values for the β- and α-phase, respectively, it turns out that the $\alpha_{transport}$ at 370 K in the α-phase is 406 µV/K higher than in the β-phase.

The $Cu_{1.8}Se$ material remains in the β-phase in the whole measurement temperature range, so can be used to compare with the $Cu_{1.99}Se$ sample in conditions, in which the latter material is in the α-phase. The Seebeck coefficient of $Cu_{1.8}Se$ at 370 K is around 180 µV/K lower than at 410 K. One can estimate the ionic Seebeck coefficient of β structure $Cu_{1.99}Se$ at 370 K (noted as $\alpha_{Cu1.99Se\beta}(370 K)$). Let's assume that:

$$\alpha_{Cu1.8Se\beta}(410K) - \alpha_{Cu1.8Se\beta}(370K)$$
$$= \alpha_{Cu1.99Se\beta}(410K) - \alpha_{Cu1.99Se\beta}(370K) \qquad (5)$$

This gives $\alpha_{Cu1.99Se\beta}(370 K)$ equal to 852 µV/K. Now, one can write:

$$\alpha_{Cu1.99Se\alpha}(370K)$$
$$= \alpha_{Cu1.99Se\beta}(370K) + \Delta_{\beta\rightarrow\alpha}\alpha_{transport} + \Delta_{\beta\rightarrow\alpha}\alpha_{presence} \qquad (6)$$

where $\Delta_{\beta\rightarrow\alpha}\alpha_{transport}$ and $\Delta_{\beta\rightarrow\alpha}\alpha_{presence}$ are the difference of transport and presence part of the Seebeck coefficient between α and β phases. These two values were discussed above, $\Delta_{\beta\rightarrow\alpha}\alpha_{transport} = +406$ µV/K and $\Delta_{\beta\rightarrow\alpha}\alpha_{presence} = -79$ µV/K.

Adding the differences in presence and transport parts calculated above, a Seebeck coefficient equal to 1179 µV/K for α-Cu$_{1.99}$Se at 370 K was obtained. This is in good agreement with the value measured in this work for this material, which is 1217 ± 107 µV/K at 370 K.

The changes of α_{ion} in the high-temperature phase are themselves unexpected. Simple calculations based on Eqs. (1) and (4) (for Cu$^+$ ions, assuming the Dulong–Petit heat capacity of these ions) suggest that the difference in ionic Seebeck coefficient across the whole temperature range should be equal to 20 µV/K, with higher values at lower temperatures.

Conclusions

The ionic Seebeck coefficient of copper selenide with Cu$_{1.99}$Se, Cu$_{1.95}$Se and Cu$_{1.8}$Se stoichiometry was measured in the phase transition temperature. Measurements were performed with $0.15\text{C}_6\text{H}_{12}\text{N}_4\text{CH}_3\text{I} + 0.85\text{CuI}$ electrolyte layers pressed with powder into a sandwich-like structure.

Above 410 K, when investigated materials are in the high-temperature phase, their ionic Seebeck coefficient was in the order of 1000 µV/K (between 900 and 1200). When the temperature decreases, the ionic Seebeck coefficient of β-Cu$_{2-\delta}$Se firstly gets higher and gradually decreases below 395 K, remaining above 900 µV/K up to 355 K, which was observed for the Cu$_{1.8}$Se sample. In the case of Cu$_{1.99}$Se, an increase in ionic thermopower is observed, when the material transforms into the α-phase. The measured difference of ionic Seebeck coefficients of the two phases matches the expected value obtained from calculated changes in the presence and transport part of the thermoelectric effect. This difference is equal to 327 µV/K at 370 K, resulting mainly from higher activation energy in the low-temperature phase. In the β-phase, the activation energy is related to hopping between lattice positions, while in the α-phase, the measured activation barrier is an apparent value resulting from both hopping and defect generation, but closer in value to the latter. This suggests that the transport part of the Seebeck coefficient is related to the activation energy regardless of its nature. The temperature dependence of Cu$_{1.95}$Se was close to that of Cu$_{1.8}$Se when the content of the β-phase was higher than about 40%, showing that the low-temperature α-phase influences the ionic Seebeck

coefficient only when having high content, due to its low ionic conductivity.

Data and code availability

The research data used in this paper are available at The Bridge of Data repository, https://doi.org/10.34808/1cn7-qt27.

Declarations

Conflict of interest   There are no conflicts to declare.

Ethical approval   Not applicable.

Supplementary Information   The online version contains supplementary material available at https://doi.org/10.1007/s10853-023-09107-w.

References

[1] Liu H, Shi X, Xu F, Zhang L, Zhang W, Chen L, Li Q, Uher C, Day T, Snyder Jeffrey G, Snyder GJ (2012), Copper ion liquid-like thermoelectrics. Nat Mater 11:422–425. https://doi.org/10.1038/nmat3273.

[2] Yu B, Liu W, Chen S, Wang HH, Wang HH, Chen G, Ren Z (2012) Thermoelectric properties of copper selenide with ordered selenium layer and disordered copper layer. Nano Energy 1:472–478. https://doi.org/10.1016/J.NANOEN.2012.02.010

[3] Di Liu W, Yang L, Chen ZG (2020) Cu2Se thermoelectrics: property, methodology, and device. Nano Today 35:100938. https://doi.org/10.1016/J.NANTOD.2020.100938

[4] Qin Y, Yang L, Wei J, Yang S, Zhang M, Wang X, Yang F (2020) Doping effect on Cu_2Se thermoelectric performance: a review. Mater 13:5704. https://doi.org/10.3390/MA13245704.

[5] Zhang Z, Zhao K, Wei TR, Qiu P, Chen L, Shi X (2020) Cu 2 Se-Based liquid-like thermoelectric materials: looking back and stepping forward. Energy Environ Sci 13:3307–3329. https://doi.org/10.1039/D0EE02072A

[6] Chakrabarti DJ, Laughlin DE (1981) The Cu-Se (Copper-Selenium) system. Bull Alloy Phase Diagrams 2:305–315. https://doi.org/10.1007/BF02868284

[7] Kang SD, Danilkin SA, Aydemir U, Avdeev M, Studer A, Snyder GJ (2016) Apparent critical phenomena in the superionic phase transition of Cu2-xSe. New J Phys 18:013024. https://doi.org/10.1088/1367-2630/18/1/013024

[8] Chen L, Liu J, Jiang C, Zhao K, Chen H, Shi X, Chen L, Sun C, Zhang S, Wang Y, Zhang Z (2019) Nanoscale behavior and manipulation of the phase transition in single-crystal Cu2Se. Adv Mater 31:1804919. https://doi.org/10.1002/adma.201804919

[9] Chrissafis K, Paraskevopoulos KM, Manolikas C (2006) Studying Cu2-xSe phase transformation through DSC examination. J Therm Anal Calorim 84:195–199. https://doi.org/10.1007/s10973-005-7169-7

[10] Tonejc A, Tonejc AM (1981) X-ray diffraction study on α ↔ β phase transition of Cu2Se. J Solid State Chem 39:259–261. https://doi.org/10.1016/0022-4596(81)90340-6

[11] Sun S, Li Y, Chen Y, Xu X, Kang L, Zhou J, Xia W, Liu S, Wang M, Jiang J, Liang A, Pei D, Zhao K, Qiu P, Shi X, Chen L, Guo Y, Wang Z, Zhang Y, Liu Z, Yang L, Chen Y (2020) Electronic origin of the enhanced thermoelectric efficiency of Cu2Se. Sci Bull 65:1888–1893. https://doi.org/10.1016/j.scib.2020.07.007

[12] Chen H, Yue Z, Ren D, Zeng H, Wei T, Zhao K, Yang R, Qiu P, Chen L, Shi X, Chen H, Yue Z, Ren D, Zeng H, Wei T, Zhao K, Qiu P, Chen L, Shi X, Yang R (2019) Thermal conductivity during phase transitions. Adv Mater 31:1806518. https://doi.org/10.1002/ADMA.201806518

[13] Byeon D, Sobota R, Hirata K, Singh S, Choi S, Adachi M, Yamamoto Y, Matsunami M, Takeuchi T (2020) Dynamical variation of carrier concentration and colossal Seebeck effect in Cu2S low-temperature phase. J Alloys Compd 826:154155. https://doi.org/10.1016/j.jallcom.2020.154155

[14] Bikkulova NN, Gorbunov VA, Akmanova GR, Kurbangulov AR, Bikkulova LV, Safargaleev DI, Nigmatullina GR, Alymov MI (2020) Ionic conductivity in copper selenides. Dokl Phys 65:265–268. https://doi.org/10.1134/S1028335820080017/TABLES/1

[15] Kumar S, Gupta MK, Goel P, Mittal R, Delaire O, Thamizhavel A, Rols S, Chaplot SL (2022) Solidlike to liquidlike behavior of Cu diffusion in superionic Cu2 X (X= S, Se): an inelastic neutron scattering and ab initio molecular dynamics investigation. Phys Rev Mater 6:055403. https://doi.org/10.1103/PHYSREVMATERIALS.6.055403/FIGURES/8/MEDIUM

[16] Callen HB (1948) The application of Onsager's reciprocal relations to thermoelectric, thermomagnetic, and galvanomagnetic effects. Phys Rev 73:1349. https://doi.org/10.1103/PhysRev.73.1349

[17] Wagner C (1972) The thermoelectric power of cells with ionic compounds involving ionic and electronic conduction. Prog Solid State Chem 7:1–37. https://doi.org/10.1016/0079-6786(72)90003-9

[18] Brown DR, Day T, Borup KA, Christensen S, Iversen BB, Snyder GJ (2013) Phase transition enhanced thermoelectric figure-of-merit in copper chalcogenides. APL Mater 1:052107. https://doi.org/10.1063/1.4827595

[19] Markov VA, Kurushkin MV, Sokolov IA (2021) Thermodiffusion of alkali ions in alkali niobophosphate glasses. Int J Appl Glas Sci 12:222–232. https://doi.org/10.1111/IJAG.15858

[20] Smith JF, Peterson DT, Smith MF (1985) An interpretation of Q* in thermotransport. J Less Common Met 106:19–26. https://doi.org/10.1016/0022-5088(85)90361-3

[21] Balapanov MK, Zinnurov IB, Akmanova GR (2006) The ionic Seebeck effect and heat of cation transfer in Cu2−δSe superionic conductors. Phys Solid State 48:1868–1871. https://doi.org/10.1134/S1063783406100076

[22] Balapanov MK, Yakshibaev RA, Mukhamed'yanov UK (2003) Ion transfer in solid solutions of Cu2Se and Ag2Se

superionic conductors. Phys Solid State 45:634–638. https://doi.org/10.1134/1.1568997.

[23] Trawiński B, Łapiński M, Kusz B (2021) The unstable thermoelectric effect in non-stoichiometric Cu2Se during the non-equilibrium phase transition. J Mater Sci 56:13705–13714

[24] Byeon D, Sobota R, Singh S, Ghodke S, Choi S, Kubo N, Adachi M, Yamamoto Y, Matsunami M, Takeuchi T (2020) Long-term stability of the Colossal Seebeck effect in metallic Cu2Se. J Electron Mater 49:2855–2861. https://doi.org/10.1007/s11664-019-07884-2

[25] Mostafa SN, Selim SR, Soliman SA, El-Lakwah FA (1989) Thermodynamic investigations on cuprous selenide, Berichte Der Bunsengesellschaft Für Phys. Chemie 93:123–128. https://doi.org/10.1002/BBPC.19890930205

[26] Nazrul Islam SMK, Mayank P, Ouyang Y, Chen J, Sagotra AK, Li M, Cortie MB, Mole R, Cazorla C, Yu D, Wang X, Robinson RA, Cortie DL (2021) Copper diffusion rates and hopping pathways in superionic Cu2Se. Acta Mater 215:117026. https://doi.org/10.1016/J.ACTAMAT.2021.117026.

[27] Horvatić M, Vučić Z (1984) DC ionic conductivity measurements on the mixed conductor Cu2-xSe. Solid State Ionics 13:117–125. https://doi.org/10.1016/0167-2738(84)90045-6

[28] Ishikawa T, Ya Miyatani S (1977) Electronic and Ionic Conduction In Cu2–δSe, Cu2–δS and Cu2–δ(Se, S). J Phys Soc Japan 42:159–167. https://doi.org/10.1143/JPSJ.42.159.